Rev. Roum. Sci. Techn.– Électrotechn. et Énerg.
Vol. **61**, *3*, pp. 278–282, Bucarest, 2016

CONTROL OF STACKED MULTICELLULAR INVERTER

SALAH HANAFI [1], MOHAMMED KARIM FELLAH[1], MOHAMMED YAICHI[2], MOHAMMED-FOUAD BENKHORIS[3]

Key words: Stacked multicellular converter (SMC), Cell, Space vector modulation (SVM), Proportional integral (PI) regulator.

The stacked multicellular dc/ac converter is a very interesting topology. But, the major problem of this structure is the imbalance of the voltage across the floating capacitors, when the input voltage changes. In this article we propose a space vector modulation (SVM) control algorithm for *N* level inverters with PI regulator. That ensures the rebalancing of the floating voltages. To validate this technique, a simulation was made under MATLAB/SIMULINK of 3x2 cells stacked multicellular dc/ac converter controlled by a SVM control with PI regulator. Simulation results show that this proposed technique is very efficient in terms of floating voltages regulation.

1. INTRODUCTION

Power electronics has known an important technological development thanks to the development of power semi-conductor and new energy conversion systems [1].

Nowadays, technological limitations of power semi-conductors limit the applications of the power converters. An isolated gate bipolar transistor (IGBT), for example, has a 4.5 kV rating. If the application requires higher voltage, an alternate topology the converter must be considered. A stacked multicell converter (SMC) represents a new solution to the problem. A SMC is a dc-ac converter for high voltage applications [2].

This configuration allows to share the total voltage and current stresses among the switches. Then, it is possible to use conventional semiconductors to handle high output power [3]. It also allows splitting the input voltage into several fractions to decrease the rate of the power switches. The SMC converter has excellent dynamic performances due the multiplication of the chopped voltage frequency and the increase of the number of levels [4]. Moreover, this topology enables to reduce significantly the energy stored in the floating capacitors by the converter, as well as the losses in the power semiconductors [5].

This significant potential of the stacked multicellular converter should be preserved. For this, its control must ensure a fast and efficient regulation of the voltages generated by the floating capacitors.

The SVM control brings important improvements (im-provement of the output signal, diminution of the THD,…) for the multilevel converters. Various recent works use the SVM strategy to control just the flying capacitor multicellular topology like [6–8]. But, this works give not a SVM algorithm generalized to *N* levels.

In this article we solve two major problems in the control of multilevel converters. Where, we propose a SVM algorithm generalized to *N* levels to control the stacked multicellular converter. And we give a simple solution for regulating the (*P*–1) floating voltages of each stack in using a PI regulator.

2. STACKED MULTICELLULAR CONVERTER

The stacked multicellular converter (SMC) appeared in the early 2000's [9].

It is constituted of an hybrid association of commutation cells (Fig. 1). In this particular case, the $P \times 2$ SMC is composed of P columns and $n = 2$ stacks. It uses Pxn commutation cells and $(P-1) \times n$ floating capacitors. This converter can generate $(P \times 2) + 1$ level. The upper stack is switched only when a positive output is required, and the lower stack is switched only when a negative output is required.

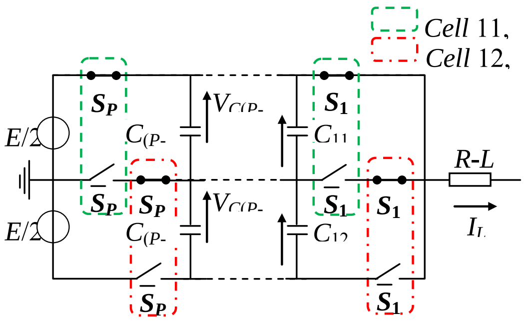

Fig. 1 – A stacked multicellular converter $P \times 2$ powering an *R-L* load.

To find the model to the instantaneous values of the SMC we considers:

- The switches are ideal (saturation voltage, leakage current, downtime and null switching time).
- The switches of the same commutation cell operate in complementary.
- The supply voltage E is constant.

Equation (1) represents the evolution of the voltage across the floating capacitors (V_{Ci1}, V_{Ci2}) for the two stacks and the evolution of the load current I_L; for a 3×2 Stacked Multicellular dc/ac converter powering an *R-L* load [9]:

$$\left|\begin{aligned} \frac{\mathrm{d}}{\mathrm{d}t}V_{C_{11}} &= \frac{S_{21}-S_{11}}{C_{11}}\cdot I_L \\ \frac{\mathrm{d}}{\mathrm{d}t}V_{C_{21}} &= \frac{S_{31}-S_{21}}{C_{21}}\cdot I_L \\ \frac{\mathrm{d}}{\mathrm{d}t}V_{C_{12}} &= \frac{S_{22}-S_{12}}{C_{12}}\cdot I_L \\ \frac{\mathrm{d}}{\mathrm{d}t}V_{C_{22}} &= \frac{S_{32}-S_{22}}{C_{22}}\cdot I_L \end{aligned}\right. , \qquad (1)$$

[1] Djillali Liabes University of Sidi Bel-Abbes, ICEPS Laboratory (Intelligent Control & Electrical Power Systems), Sidi Bel-Abbes, Algeria, E-mail: sal_hanafi@outlook.com
[2] Research Unit in Renewable Energies in Saharan Medium URER/MS Adrar, Algeria
[3] University of Nantes at Saint Nazaire, IREENA Laboratory (Institut de Recherche en Electronique et Electrotechnique de Nantes Atlantique), France

$$\left|\begin{array}{l}\dfrac{\mathrm{d}}{\mathrm{d}t}I_L=-\dfrac{R_L}{L_L}I_L+\dfrac{S_{11}-S_{21}}{L_L}V_{C_{11}}+\dfrac{S_{21}-S_{31}}{L_L}V_{C_{21}}\\ +\dfrac{S_{12}-S_{22}}{L_L}V_{C_{12}}+\dfrac{S_{22}-S_{32}}{L_L}V_{C_{22}}+\dfrac{S_{31}E_1}{L_L}\\ +\dfrac{(S_{32}-1)E_2}{L_L}\end{array}\right. . \quad (1)$$

From equations (1) we can define the state equation of this system:

$$\dot{X}=A\cdot X+B(X)\cdot S\,, \quad (2)$$

where the instantaneous values model of the SMC 3 × 2 is as follows:

$$X=\begin{bmatrix}V_{C_{11}} & V_{C_{21}} & 0 & V_{C_{12}} & V_{C_{22}} & I_L\end{bmatrix}^{\mathrm{T}},$$

$$S=\begin{bmatrix}S_{11} & S_{21} & S_{31} & S_{12} & S_{22} & S_{32}\end{bmatrix}^{\mathrm{T}},$$

$$B(X)=\begin{pmatrix}-\dfrac{I_L}{C_{11}} & \dfrac{I_L}{C_{11}} & 0 & 0 & 0 & 0\\ 0 & -\dfrac{I_L}{C_{21}} & \dfrac{I_L}{C_{21}} & 0 & 0 & 0\\ 0 & 0 & -\dfrac{I_L}{C_{12}} & \dfrac{I_L}{C_{12}} & 0 & 0\\ 0 & 0 & 0 & 0 & -\dfrac{I_L}{C_{22}} & \dfrac{I_L}{C_{22}}\\ \dfrac{V_{C_{11}}}{L_L} & \dfrac{V_{C_{21}}-V_{C_{11}}}{L_L} & \dfrac{E_1-V_{C_{21}}}{L_L} & \dfrac{V_{C_{12}}}{L_L} & \dfrac{V_{C_{22}}-V_{C_{12}}}{L_L} & \dfrac{E_2-V_{C_{22}}}{L_L}\end{pmatrix},$$

$$A=\begin{pmatrix}0 & 0 & 0 & 0 & 0 & 0\\ 0 & 0 & 0 & 0 & 0 & 0\\ 0 & 0 & 0 & 0 & 0 & 0\\ 0 & 0 & 0 & 0 & 0 & 0\\ 0 & 0 & 0 & 0 & 0 & 0\\ 0 & 0 & 0 & 0 & 0 & -\dfrac{R_L}{L_L}-\dfrac{E_2}{L_L\cdot I_L}\end{pmatrix}.$$

3. SPACE VECTOR MODULATION CONTROL WITH PI REGULATOR

The space vector modulation (SVM) offers the significant flexibility to optimize the switching diagrams. But, the determination of the switch position of the SVM is difficult when the level number changes.

We are going to present a very efficient algorithm of SVM for N level inverters. This algorithm is independent of the number of levels and is based on three steps (coordinate transformation, detection of closest three vector, calculating of the switches commutation time).

Let's compare the voltage space vectors of the two inverters of three and four levels shown in Fig. 2.

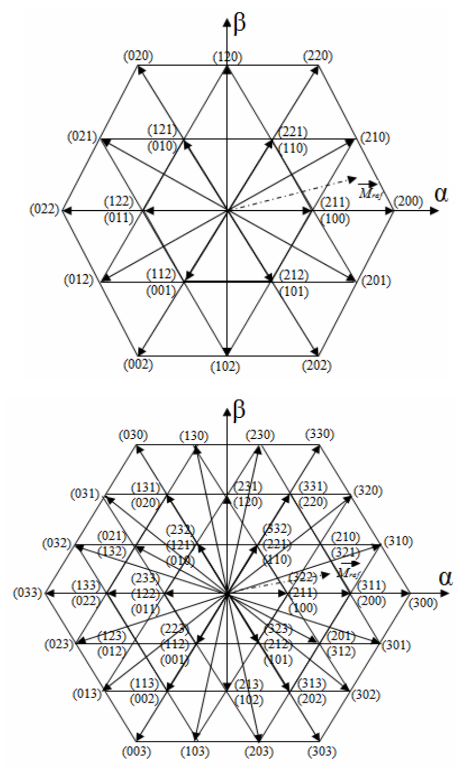

Fig. 2 – Switching vectors of inverters of three and four levels respectively.

The output voltages of the inverter are represented by a hexagonal structure model. Let's start with the simplest hexagon which corresponds to the two-level inverters. Each new level adds a triangular rings equilateral constituting a new hexagon formed of voltage vectors. This observation serves as a basis for establishment of new algorithms.

From there, the hexagons structure regularity is used to guarantee an efficiently representation of the vectors in the plane, and also to generalize the SVM algorithm. From there, we can represent the switching vectors and the reference vector in a new base (g, h), where a set of non-orthogonal vectors can be chosen. This base changing is defined by [10] (U represents the dc voltage):

$$\left\{\vec{g}(v_{ab},v_{bc},v_{ca}),\vec{h}(v_{ab},v_{bc},v_{ca})\right\}=\left\{\begin{bmatrix}U\\0\\-U\end{bmatrix},\begin{bmatrix}0\\U\\-U\end{bmatrix}\right\}. \quad (3)$$

The first step in the algorithm is the transformation of the reference vector V_{ref} from the line-to-line coordinate system (equation (5)) into a two-dimensional coordinate system (g, h) in using equation (4). This transformation normalizes also the reference vector with the length of the base vector

$$\vec{V}_{ref\,(g,h)}=T\vec{V}_{ref\,(v_{ab},v_{bc},v_{ca})} \quad (4)$$

$$\vec{V}_s=\begin{bmatrix}v_{ab}\\v_{bc}\\v_{ca}\end{bmatrix}, \quad (5)$$

where $\vec{V}_s$ is the voltage vector between phases represented in a three dimensional Euclidean space, with

$$\begin{bmatrix} V_a \\ V_b \\ V_c \end{bmatrix} = r.\begin{bmatrix} \cos(\omega t) \\ \cos(\omega t - (2\pi/3)) \\ \cos(\omega t + (2\pi/3)) \end{bmatrix}. \quad (6)$$

$$T = \frac{1}{3}.\frac{N-1}{2}.\begin{bmatrix} 2 & -1 & -1 \\ -1 & 2 & -1 \end{bmatrix}. \quad (7)$$

Figure 3 shows all the switching vectors of a three-level inverter, with the corresponding switching states in the new coordinate system (g, h) (M_{ref} is the switching state vector).

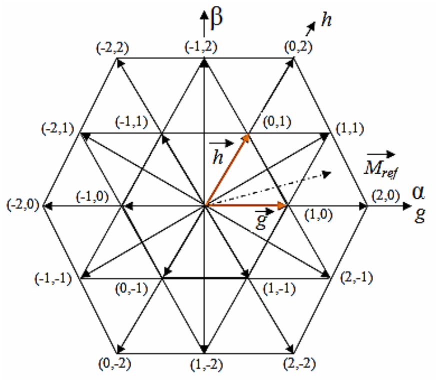

Fig. 3 – Switching state vectors of a three-level inverter in (g, h) system.

In the field of control functioning in a two-phase coordinate system, as is the case in most modern controls of alternative machines, this can be realized in using a transformation of the reference vector V_{ref} from (α, β) coordinate system into a two-dimensional coordinate system (g, h). The result of the transformation matrix is:

$$\vec{V}_{ref\,(g,h)} = T_1 \vec{V}_{ref\,(\alpha,\beta)}. \quad (8)$$

$$T_1 = \frac{3}{2}.\frac{N-1}{2}.\begin{bmatrix} 1 & -1/\sqrt{3} \\ 0 & 2/\sqrt{2} \end{bmatrix}. \quad (9)$$

The fact that all the switching vectors have integer coordinates allow us to identify simply the four vectors nearest to the reference vector, while, the vectors that the coordinates are a combinations of upper and lower rounded integer values of the reference vector coordinates are calculated as follows [10]:

$$\vec{V}_{ul} = \begin{bmatrix} \lceil V_{refg} \rceil \\ \lfloor V_{refh} \rfloor \end{bmatrix},\ \vec{V}_{lu} = \begin{bmatrix} \lfloor V_{refg} \rfloor \\ \lceil V_{refh} \rceil \end{bmatrix},$$
$$\vec{V}_{uu} = \begin{bmatrix} \lceil V_{refg} \rceil \\ \lceil V_{refh} \rceil \end{bmatrix},\ \vec{V}_{ll} = \begin{bmatrix} \lfloor V_{refg} \rfloor \\ \lfloor V_{refh} \rfloor \end{bmatrix}, \quad (10)$$

with $\lceil V_{ref} \rceil, \lfloor V_{ref} \rfloor$ being the superior and inferior rounded value of V_{ref} respectively.

So, we obtain an equal-sided parallelogram formed by the endpoints of the closest four vectors, and the diagonal connecting the vectors V_{ul} and V_{lu} divided it into two equilateral triangles. The three closest vectors are always constituted of two fixed vectors which are V_{ul} and V_{lu}. Consequently, from the two remaining vectors situated on the same side of the diagonal, we chose the third closest vector [11], where we evaluate the sign of the expression (11):

$$V_{refg} + V_{refh} - (V_{ulg} + V_{ulh}). \quad (11)$$

Equation (12) and Fig. 4 explain how the third closest vector (TCV) is chosen (second step).

$$\begin{aligned} &\text{If}: \quad V_{refg} + V_{refh} - (V_{ulg} + V_{ulh}) > 0, \\ &\Rightarrow \quad V_{uu} \ \text{ is the TCV}, \\ &\text{If}: \quad V_{refg} + V_{refh} - (V_{ulg} + V_{ulh}) < 0. \\ &\Rightarrow \quad V_{ll} \ \text{ is the TCV}. \end{aligned} \quad (12)$$

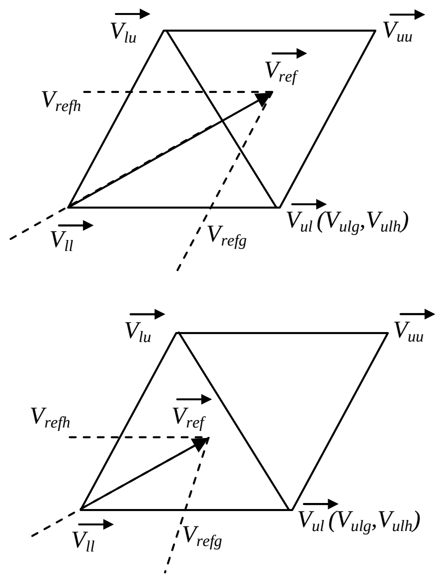

Fig. 4 – Two different cases of the position of the reference vector, using the same four closest vectors.

Now, the identification of the three closest vectors for the N levels inverters is completed. So, we can found the commutation times of the switches by solving (13) and (14) (third step):

$$\vec{V}_{ref} = (d_1.\vec{V}_1 + d_2.\vec{V}_2 + d_3.\vec{V}_3). \quad (13)$$

$$d_1 + d_2 + d_3 = 1, \quad (14)$$

with

$$\vec{V}_1 = \vec{V}_{ul};\ \vec{V}_2 = \vec{V}_{lu};\ \vec{V}_3 = \vec{V}_{ll} \ \text{ or } \ \vec{V}_3 = \vec{V}_{uu}. \quad (15)$$

It's noted that, the switching-state vectors have always an integer coordinates. So, the solutions are the fractional parts of the V_{ref} coordinates [11].

$$\text{If}: \ \vec{V}_3 = \vec{V}_{ll} \quad \text{so} \quad \begin{cases} d_{ul} = V_{refg} - V_{llg} \\ d_{lu} = V_{refh} - V_{llh} \\ d_{ll} = 1 - d_{ul} - d_{lu} \end{cases}, \quad (16)$$

or

$$\text{If}: \ \vec{V}_3 = \vec{V}_{uu} \quad \text{so} \quad \begin{cases} d_{ul} = V_{refh} - V_{uuh} \\ d_{lu} = V_{refg} - V_{uug} \\ d_{uu} = 1 - d_{ul} - d_{lu} \end{cases}. \quad (17)$$

In looking at equation (1) that manages the evolution of the floating voltages, we can deduce that there are two parameters that can be used to control the V_{Ci1} or V_{Ci2}; these parameters are the load current (I_L) and the control signals

(S_{i1}, $S_{(i+1)1}$ and S_{i2}, $S_{(i+1)2}$). The use of the control signals for regulating the floating voltages complicates the SVM program because it requires a lot of calculation. For there, we will add a PI regulator for regulating the floating voltages in using the load current I_L to simplify the SVM program (Fig. 5).

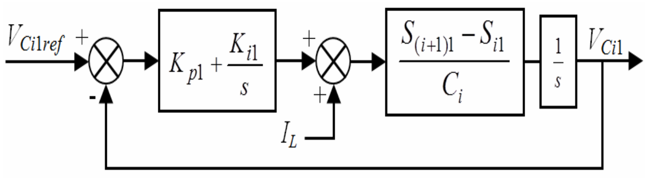

Fig. 5 – Regulation loop for the floating voltages.

4. RESULTS

The studied system is composed of 3×2 SMC dc/ac converter, supplying an *R-L* load, controlled by space vector modulation control with PI regulator for regulating the floating voltages (Fig. 6). This system is simulated under MATLAB / SIMULINK.

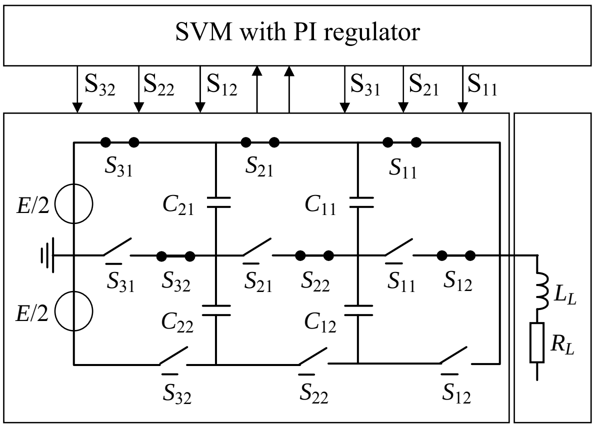

Fig. 6 – Studied system.

Table (1) gives the different parameters used in this simulation.

Table 1

Parameters used in simulation

Parameters	Values
E (dc voltage)	1500 V
C (Floating capacitor)	40 µF
L_L (Inductance)	1 mH
R_L (Resistance)	10 Ω
f_c (Cutting frequency)	26 kHz
r (Modulation rate)	0.8
m (Modulation index)	520
K_p	50
K_i	5

In first, this system is simulated without regulation to see the reaction of the floating voltages, load current and the output voltage (Fig. 7). Then, we introduce the PI regulator to show the efficiency of the proposed regulation (Fig. 8). It should be noted that, the floating voltages are measured directly.

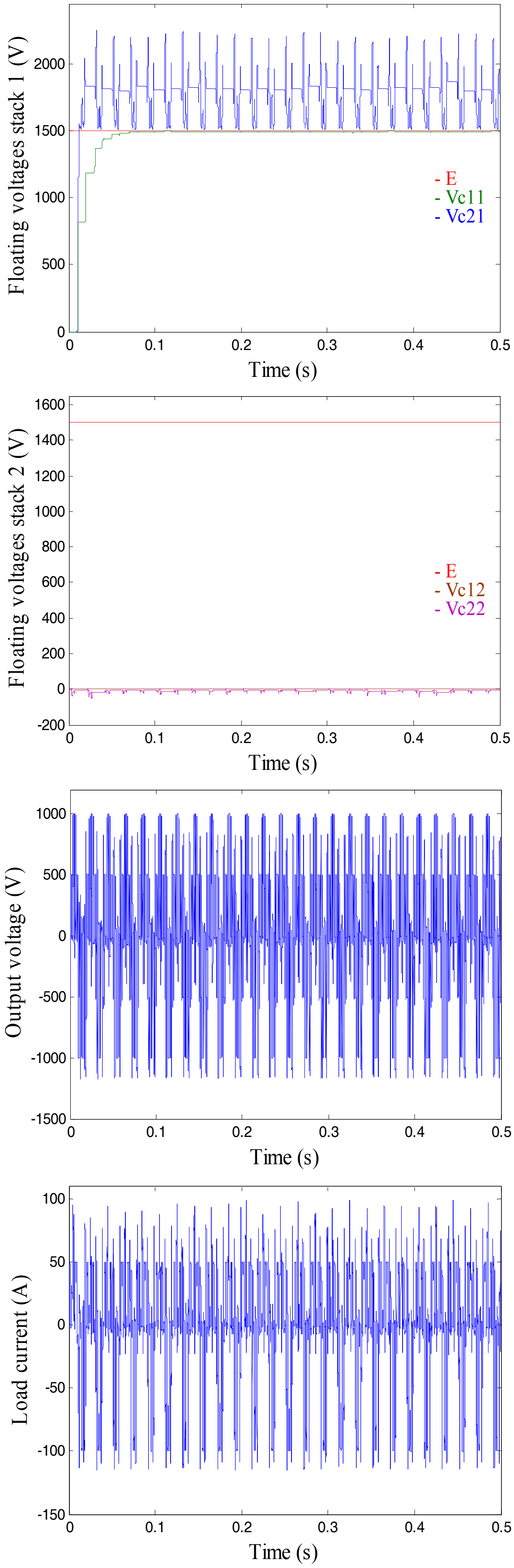

Fig. 7 – Representation of the results obtained without regulation.

As we can see in Fig. 7 the floating voltages are unbalanced, which produces a loss of the converter performances (the output voltage doesn't reach all its levels, the voltage and current are rich in harmonics…).

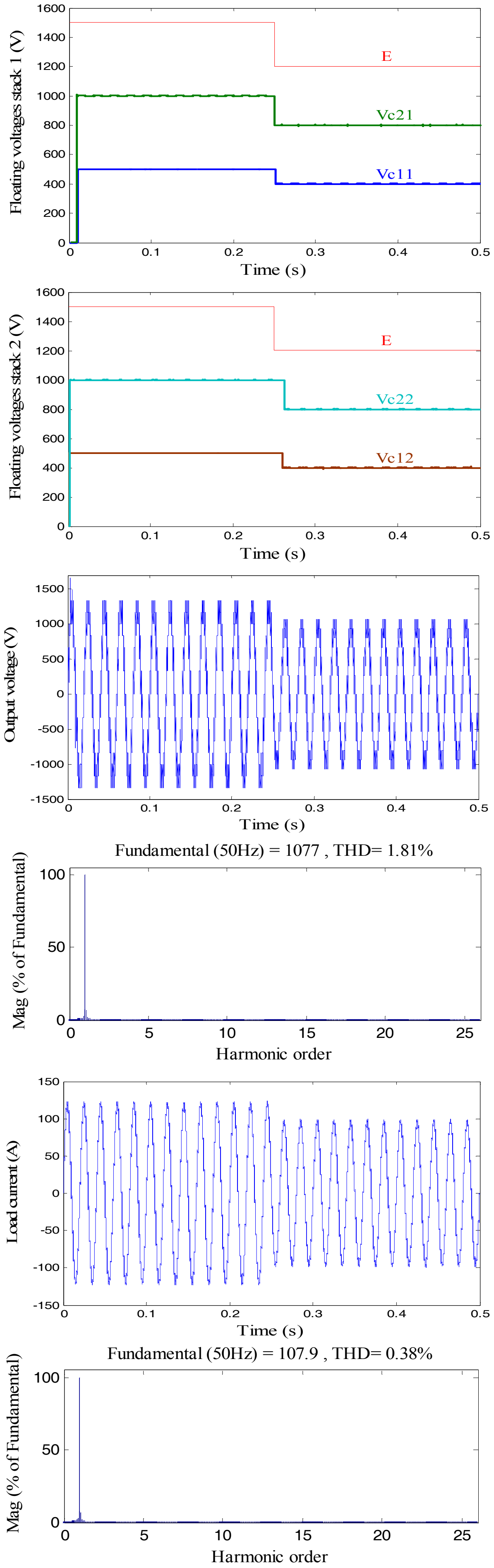

Fig. 8 – Representation of the results obtained with regulation.

In Fig. 8, it can be seen that, there is no transitional scheme and the floating voltages are balanced. At $t = 0.25$ s, we simulate a voltage drop, where, we decrease the converter supply voltage E of 300 V. As results, the floating voltages are balanced and follow this change quickly, the output voltage reaches all its levels and its output signal is not rich in harmonics (V_o THD = 1.81 %). The load current is almost sinusoidal periodic signal (I_L THD = 0.38 %).

5. CONCLUSION

Two major problems are solved in this article. The first one is the complexity to realize a SVM algorithm for controlling multilevel converters when the level is high. The second one concerns the imbalance of the floating voltages. As solution, we presented a generalized SVM algorithm (generalized algorithm for multilevel inverters with any number of levels) to control the SMC dc/ac converter. Then, we proposed a regulation of the floating voltages with PI regulator.

The SVM control with PI regulator has given a good regulation of the floating voltages with a minimum response time and improve the output waveforms of the converter in particular the harmonic content.

Received on September 25, 2015

REFERENCES

1. K. Benmansour, A. Benalia, M. Djemai, J. Leon, *Hybrid control of a multicellular converter* (Elsevier), Nonlinear analysis: Hybrid systems, **1**, *1*, pp. 16–29 (2007).
2. L. Delmas, G. Gateau, T.A. Meynard, H. Foch, *Stacked Multicell converter (SMC): Control and Natural Balancing*, Power Electronics Specialists Conference (PESC 02), IEEE 33rd Annual, **2**, 23–27 June 2002, pp. 689–694.
3. J. Courault, O. Lapierre, J.L. Pouliquen, *Industrial interest of mul-tilevel converters*, European Power Electronics Conference, Lausanne-Switzerland, Sept. 7–9, 1999.
4. G. Gateau, T.A. Meynard, H. Foch, *Stacked Multicell Converter (SMC): Topology and control*, 9th European Conference on Power Electronics and Applications (EPE'2001), Graz, Austria, 2001, pp. 405–410.
5. A. M. Lienhardt, G. Gateau, T.A. Meynard, *Stacked Multicell Converter (SMC): Reconstruction of flying capacitor voltages*, IEEE Industrial Electronics Conference, 2005, pp. 691–696.
6. F. Salinas, M.A. González, M.F. Escalante, *New Voltage Balancing Strategy for Flying Capacitor Multilevel Converters*, IEEE Power Electronics Congress (CIEP), Aug. 2010, pp. 185–190.
7. S. Choi, M. Saeedifard, *Capacitor Voltage Balancing of Flying Capacitor Multilevel Converters by Space Vector PWM*, IEEE Trans. on Power Delivery, **27**, *3*, pp. 1154–1161 (2012).
8. M. Arasteh, A. Abrishamifar, J. Dolatabadi, *Fast SVM for a Five Level Flying Capacitor Drive with Overvoltage Reduction*, IEEE Power Electronics, Drive Systems and Technologies Conference, Feb 2013, pp. 188–192.
9. S. Hanafi, M.K. Fellah, M. Yaichi, M.F Benkhoris, *Nonlinear feedback decoupling control applied to stacked multicellular converter*, Rev. Roum. Sci. Techn. – Électrotechn. et Énerg., **59**, *1*, pp. 97–106 (2014).
10. N. Celanovic. *Space vector modulation and control of multilevel converters*, PhD thesis, Virginia Polytechnic Institute, USA, 2000.
11. N. Celanovic, D. Boroyevich, *A fast space-vector modulation algorithm for multilevel three-phase converters*, IEEE Industry Applications Conference, **37**, *2*, pp. 637–641 (2001).